Chapter 9 Solar energy monitoring system using a SEPIC converter for possible application in Nanosatellites

Capítulo 9 Sistema de Monitoreo de energía solar utilizando un convertidor SEPIC para posible aplicación en Nanosatélites

JIMÉNEZ-JUÁREZ, Josefina[1]†*, CASTILLO-BECERRIL, Brenda[1], BALDERAS-PÉREZ, Karina[2] and MASTACHE-MASTACHE, Jorge Edmundo[2,3]

[1]*Estudiante CUI, Facultad de Ingeniería*
[2]*Universidad de Ixtlahuaca CUI, Facultad de Ingeniería*
[3]*TecNM/Tecnológico de Estudios Superiores de Jocotitlán*

ID 1st Author: *Josefina, Jiménez-Juárez* / **ORC ID**: 0009-0006-5125-8468

ID 1st Co-author: *Brenda, Castillo-Becerril* / **ORC ID**: 0009-0007-2513-627X

ID 2nd Co-author: *Karina, Balderas-Pérez* / **ORC ID**: 0009-0002-0265-1272

ID 3rd Co-author: *Jorge Edmundo, Mastache-Mastache* / **ORC ID**: 0000-0001-6104-6764, **CVU CONAHCYT ID**: 544943

DOI: 10.35429/H.2023.8.117.141

*josefina.jimenez@uicui.edu.mx

A. Marroquín, L. Castillo, J. Olivare sand G.Morado (Coord) Engineering Sciences and Applications. Handbooks-©ECORFAN-México, Querétaro, 2023.

Abstract

Nanosatellites are mobile objects that orbit the Earth and are distinguished by their size and solar energy source. They consist of two main parts: the payload, which is the main reason for completing the mission, and the platform, which consists of the subsystems that enable proper operation. The most important subsystem is the electrical system (EPS), which is responsible for distributing power to the various modules and converting the energy produced by the energy recovery system. However, there are also factors that cause conversion losses, so there is an opportunity to develop solar energy monitoring systems using SEPIC converters. In this research, a monitoring system was developed that included multiple stages such as solar cell module, SEPIC converter and PWM control to emulate their behavior individually and collectively. From a certain point of view, we analyzed the parts used in the converter, evaluated the electrical circuit of the solar cell array and the SEPIC converter with variable power and the solar cells through simulation, and then performed tests in a physical environment. The monitoring system uses computer tools to measure the input and output data of the converter, saving the data in Excel software to create performance graphs.

Nanosatellites, SEPIC Converters, PWM Control, Electrical system, **Monitoring system**

Resumen

Los nanosatélites son objetos móviles que orbitan alrededor de la Tierra y se distinguen por su tamaño y su fuente de energía solar. Constan de dos partes principales: la carga útil, que es la principal razón para llevar a cabo la misión, y la plataforma, formada por los subsistemas que permiten su correcto funcionamiento. El subsistema más importante es el sistema eléctrico (EPS), que se encarga de distribuir la energía a los distintos módulos y de convertir la energía producida por el sistema de recuperación de energía. Sin embargo, también existen factores que provocan pérdidas de conversión, por lo que existe la oportunidad de desarrollar sistemas de monitorización de la energía solar utilizando convertidores SEPIC. En esta investigación, se desarrolló un sistema de monitorización que incluía múltiples etapas como el módulo de células solares, el convertidor SEPIC y el control PWM para emular su comportamiento de forma individual y colectiva. Desde cierto punto de vista, analizamos las piezas utilizadas en el convertidor, evaluamos el circuito eléctrico del conjunto de células solares y el convertidor SEPIC con potencia variable y las células solares mediante simulación, y después realizamos pruebas en un entorno físico. El sistema de monitorización utiliza herramientas informáticas para medir los datos de entrada y salida del convertidor, guardando los datos en el software Excel para crear gráficos de rendimiento.

Nanosatélites, convertidores SEPIC, control PWM, sistema eléctrico, Sistema de monitorización

1. Introduction

Currently, artificial satellites exist indirectly in people's lives, although artificial satellites were created in 1957, they have evolved over the years, improving their functions and dimensions (Patel, 2004). In response to these changes, small satellites have been developed that belong to a particular type known as nanosatellites due to their dimensions. Nanosatellites are designed to allow the reception and transmission of information to any part of the world, in addition to providing functions such as heat dissipation, position and motion correction and temperature regulation, the most common applications used in small satellites include telephony, weather, communications and military applications (Fernandez, 2004). Similarly, nanosatellites can be deployed in space individually or as part of a network of interconnected nanosatellites to perform specific functions defined as payloads.

All nanosatellites have built-in photovoltaic systems that allow them to capture solar energy in space (Abella, 2021). However, because they are exposed to much harsher environmental conditions than the Earth's surface, they are equipped with a power energy system (EPS) with direct current to direct current (DC-DC) power conversion that take into account factors such as power consumption, mission and life cycle of the nanosatellite (Tamasi, 2003).

However, the amount of energy available to nanosatellite solar cells depends on the irradiance and temperature of the sun. At low solar intensities, the energy conversion within the electrical system can cause losses in the life cycle, and the energy recovered is not constant and is affected by factors such as rotational motion and partial shading. These factors can cause energy imbalances in nanosatellites, which can eventually exhaust the energy to operate and become space debris.

Therefore, we have developed a SEPIC-type DC-DC converter design characterized by its ability to provide a non-inverting output voltage and maintain a minimum input-output ripple, allowing to obtain an output of higher voltage and equal or lower than the input.

The purpose of this research was to obtain information on the maximum energy recovery values of solar cells and the performance of SEPIC converters. The methodology, design and simulation used to analyze the exact converter components and solar module properties are presented. In addition, the behavior of a series array of solar cells acting as the main power source for the converter is simulated. The physical results of the implementation of the converter with the control stage and the solar cell module are observed in the results, likewise this work can lay the groundwork for future research topics related to the efficiency of DC-DC converters, the effects of partial shading in moving nanosatellites, energy recovery in space, etc.

2. Metodology

In the present work a solar energy monitoring system capable of collecting and storing the input and output data from the SEPIC converter will be addressed, considering some parts such as a solar cell module and a PWM control, as a load for the design of the energy recovery system a possible application in Nanosatellites is considered. These parts are interrelated with the objective of capturing the maximum amount of energy coming from four solar cells, connected in series to operate a SEPIC converter controlled by PWM proportional duty cycle modulation.

The methodology to be followed is a sequence of steps described below, starting with an analysis of the load and system requirements that determine the reasons and effects of energy harvesting, which determines the model of the solar cells to be used. After determining the input source, an analytical analysis of the constituent elements of the SEPIC converter was performed.

Subsequently, the design and simulation of the solar cells and the SEPIC converter was carried out using PSIM Version 9.1 and Proteus Version 8.12 software. In PSIM, the electrical circuits of the solar cell array and the behavior of the SEPIC converter in its two operating modes known as elevator and reducer in continuous conduction mode were evaluated by simulation, using four solar cells as input source. A PWM controller with an integrated SEPIC converter was designed and evaluated in Proteus to monitor its two operating modes. At the end of the simulation, the physical and functional construction of the SEPIC converter was carried out by performing experiments with a variable power supply and a series array of solar cells, and an IT monitoring system was designed to test the operation of the SEPIC converter and monitor the variable conditions throughout the day

3. Design and simulation

The solar energy monitoring system using a SEPIC converter is composed of different stages which conclude to a main objective which is based on a possible application in nanosatellites.

Figure 1 Design stages of a SEPIC converter in draw.io

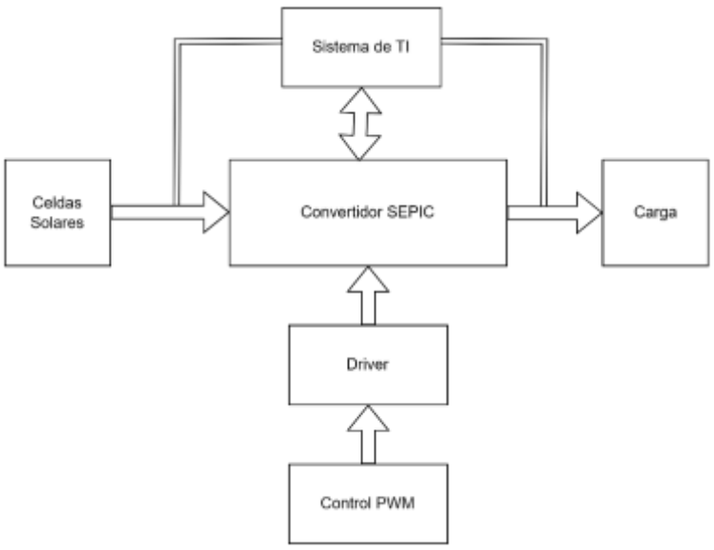

Source: Own Elaboration

– The first stage consists of a solar cell module, which serves to capture light radiation by the impact of photons on the cell surface (Céspedes, 2012), used as the main energy source for the converter.

– The PWM control stage is a modulation technique generated by the TL494 element that compares two signals, the internal tracker reference signal and the capacitor charge/discharge signal, to generate a pulse signal. The signal is internally coupled to the IR2184 driver, which is responsible for regulating the current to start the internal MOSFET of the SEPIC converter.

– The SEPIC converter in addition to taking into account the input voltage of the solar cell, is responsible for converting the continuous voltage to another voltage level of higher or lower value (Montero, 2013), depending on the operating conditions of the PWM control, allowing to observe the behavior in its static mode.

– The IT system in use can sample the SEPIC converter over a period of time, using software and hardware components that read measurements from the converter and store the data for later use.

– Charging is a target for nanosatellite missions, i.e., a device or tool to which power is supplied (Space, 2020). In the SEPIC converter design, the load is emulated as a resistor.

The above steps require analysis, design and simulation processes, which are described below.

3.1 Solar cell selection

The objective of solar cells is to feed the systems of a nanosatellite considering some criteria of efficiency, radiation resistance, dimensions and weight, as well as capacity to withstand shocks and vibrations in space (Plá, 2017), the main materials used in space photovoltaic devices are triple junction, some examples are GaInP and GaAs/Ge (Saucedo, 2016).

To characterize the cells, an analysis of the physical parameters corresponding to their data sheets was developed, which are presented in Table 1, where the open circuit voltage (V_{OC}), short circuit current (I_{SC}), maximum power voltage (V_{mpp}ó V_{mp}) were evaluated, maximum power current (I_{mpp} ó I), conversion efficiency (η), fill factor (FF) and the ratio between the maximum power generated by the cell and the product$I_{SC}V_{OC}$,, these parameters were considered for the selection of suitable SM141K10LV cells for powering the SEPIC converter.

Table 1 SM141K10LV switchgear specifications

Symbol	Cell Parameter	Typical Ratings	Units
V_{OC}	Open circuit voltage	6.91	V
I_{SC}	Short circuit current	58.6	mA
V_{mpp}	Voltage at max. power point	5.58	V
I_{mpp}	Current at max. Power point	55.1	mA
P_{mpp}	Máximum peak power	307	mW
FF	Fill factor	> 70	%
η	Solar cell efficiency	25	%
$\Delta V_{OC}/\Delta T$	Open circuit voltage temp. Coefficient	-17.4	mV/K
$\Delta I_{SC}/\Delta T$	Max power temp. Coefficient	26.5	uA/K
S	Irradiancia	1000	W/m^2
T	Temperatura	1 a 25	°C

Source: Own Elaboration

A series connection of four solar cells as input source was analyzed and the schematic diagram shown in Figure 2 was created in PSIM to characterize the SM141K10LV cell.

Figure 2 Series arrangement of SM141K10LV cells in PSIM

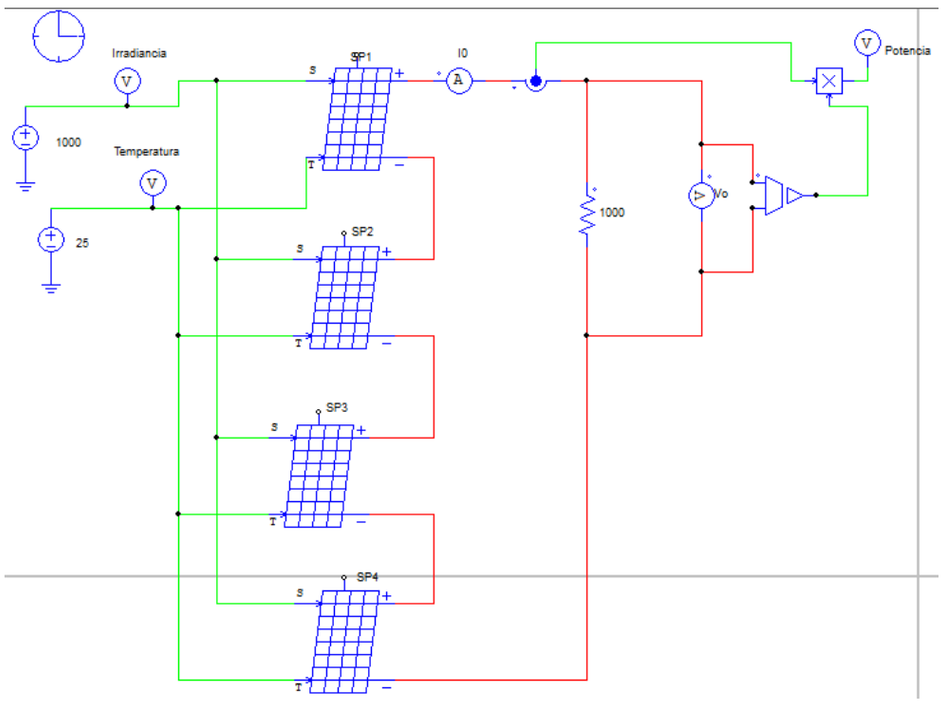

Source: Own Elaboration

Using PSIM's Physical model tool, the electrical behavior of the cells was simulated under ideal conditions of 1000 W/m^2 and an average temperature of 25°C. With the help of its data sheet, the following parameters shown in Table 1 were defined. Consequently, the current-voltage and power-voltage characteristic curves of the cell array were obtained, as shown in Figure 3, obtaining the values of maximum power (($P_{máx}$)) of 1.43W, maximum current (I_{max}) of 0.05 and maximum voltage (V_{max}) of 26.91V.

Figure 3 Physical model with 4 cells in PSIM

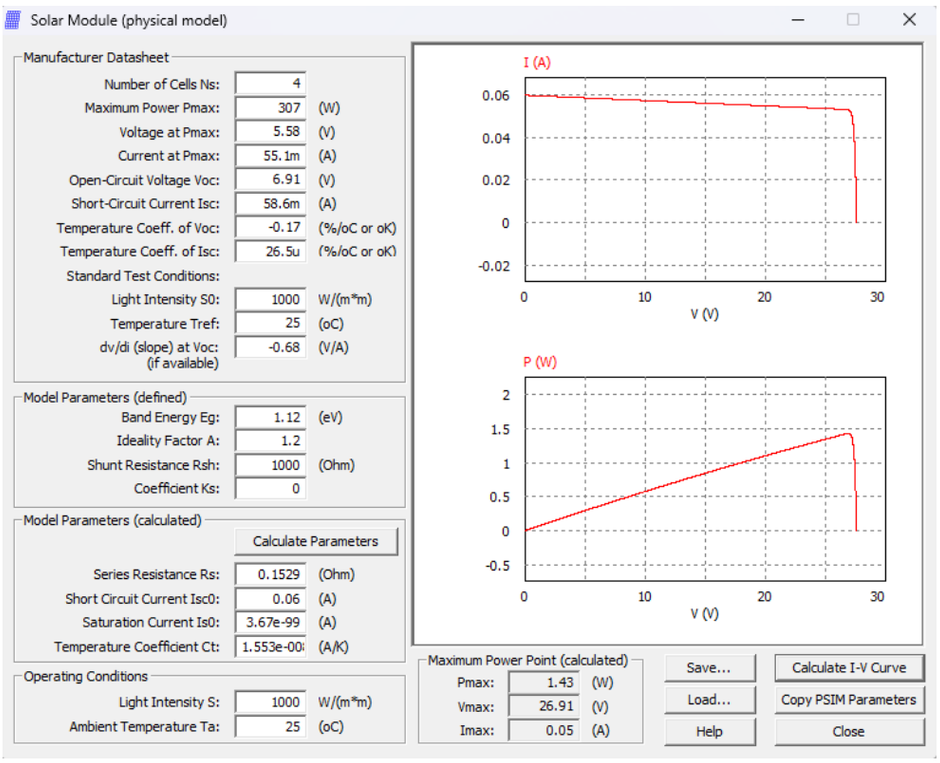

Source: Own Elaboration

3.2 Design of the PWM control stage

Proteus software was used to emulate the converter behavior. This requires a modulation technique that controls the power delivered to the load and allows the converter to maintain a steady state mode of operation.

As shown in Figure 4, the control stage was implemented with a PWM modulation technique using a TL494 circuit coupled through an IR2184 gate driver as an enabling device for the MOSFET of the SEPIC converter.

Figure 4 Schematic diagram of PWM control in Proteus

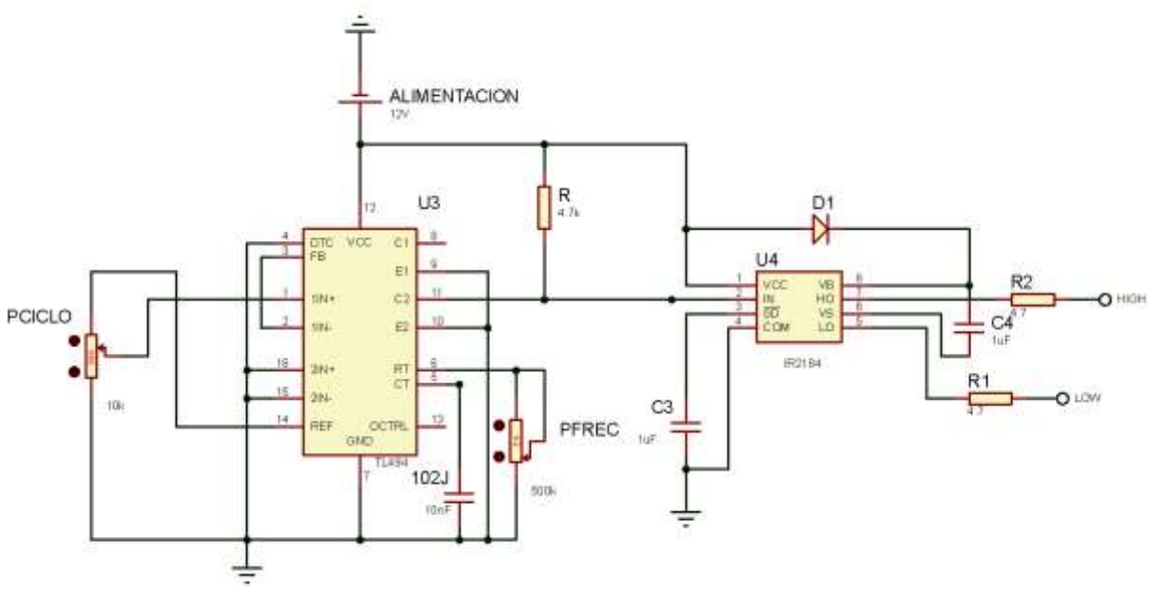

Source: Own Elaboration

The variable resistance values on pins 1,14 and 6 were adjusted to observe the duty cycle, frequency and power of the controller, for both operation modes, and a frequency of 100 kHz was also determined.

Figure 5 PWM control in the rising state in Proteus

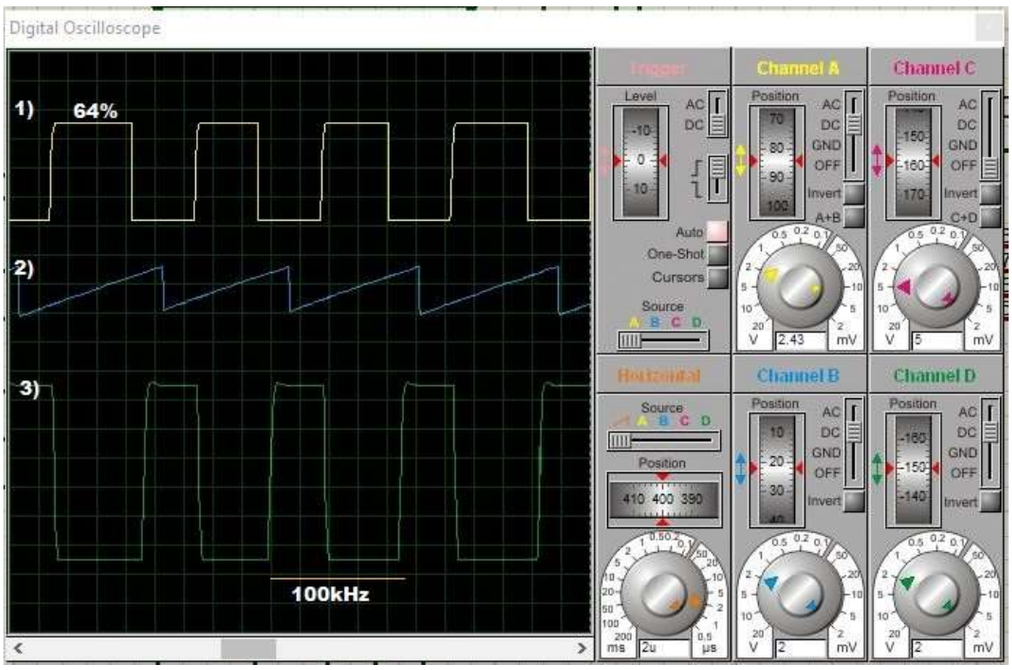

Source: Own Elaboration

As shown in Figure 5 in step-up mode, three signals are represented, the first yellow signal comes from the TL494 output with a duty cycle of 64%, the sawtooth wave is generated from the resistor-capacitor ratio and the third green signal is from the low side (LOW) of the IR2184 controller.

Figure 6 PWM control in reducing state in Proteus

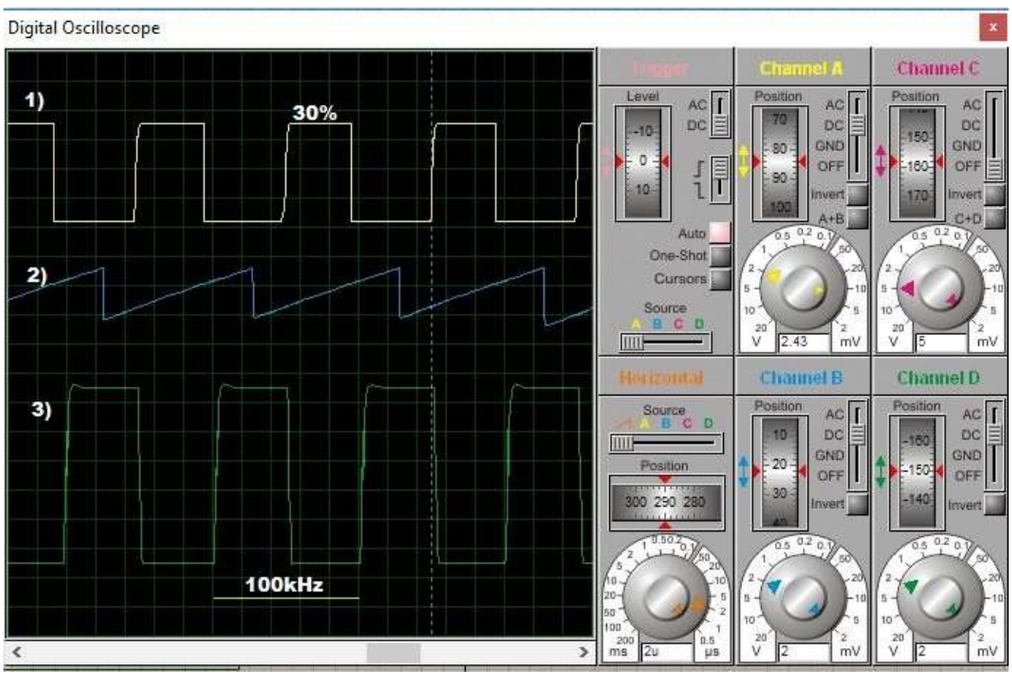

Source: Own Elaboration

In Figure 6, the first and third signals have the same duty cycle in derating mode with a value of 30%, but the yellow signal belongs to the TL494 output and the green signal belongs to the lower output of the controller.

3.3 SEPIC converter design

The purpose of a SEPIC DC-DC converter is to convert a DC voltage to a voltage level of different value, higher or lower, depending on the operating conditions of the PWM control (Flores, 2017).

In the design of the SEPIC converter, a calculation of the elements that compose the SEPIC converter was developed using the input parameters of the solar cell to determine the maximum power of the recovery system. The parameters corresponding to the converter were calculated according to Table 2 based on the design of the converter in continuous driving mode (Lopez, 2018).

Table 2 Equations and characteristic parameters of the components

Components/Parameters	Equation	Where:
Duty cycle	$D = \frac{V_o}{V_{in}+V_o}$	$V_o =$ Output voltage in Volts (V). $I_o =$ Average output current in Amperes (A) $R_o =$ Output resistance or load (Ω=V/A) $f =$ Frecuency (Hz) $D =$ Duty cycle $\Delta V_{C1} =$ Voltage ripple of the first capacitor in Volts (V). $\Delta V_{C2} =$ Voltage ripple of the second capacitor in Volts (V). $\Delta i_{L_1} =$ Current swing of the first inductor in Amperes (A). $\Delta i_{L_2} =$ Current curl of the second inductor in Amperes (A). $L_1, L_2 =$ Inductors in Hertz $((V * s/A)$ $V_{in} =$ Input voltage in Volt Volts (V)
Inductor 1	$L_1 = \frac{V_{in}D}{\Delta i_{L_1} f}$	
Inductor 2	$L_2 = \frac{V_{in}D}{\Delta i_{L_2} f}$	
Load	$R_o = \frac{V_o}{I_o}$	
Capacitor 1	$C_1 = \frac{V_o D}{\Delta V_{C1} R_o f}$	
Capacitor 2	$C_2 = \frac{V_o D}{\Delta V_{C2} R_o f}$	

Source: Own Elaboration

Using Table 2, component estimation was carried out, under step-up and step-down mode conditions with an input voltage provided by the solar cell series array of approximately 27V for both modes and a step-down output voltage (V_{out}) of 12V and step-up of 48V. In addition to considering recommended parameters such as a frequency of 100 *kHz*, ΔV_{c1} of 100mV and ΔV_{c2} of $10mV$, determining in Table 3 the construction components of a SEPIC converter.

Table 3 Definition of components

Components	Elevator	Reducer
Duty cycle	0.30	0.64
Capacitor 1	$3.69\mu F$	$1.92\mu F$
Capacitor 2	$36.90\mu F$	$19.2\mu F$
Inductor 1	$4.90mH$	$10mH$
Inductor 2	$2.19mH$	$19mH$
Load	97.56Ω	1.6kΩ

Source: Own Elaboration.

The definition of the components allowed the comparison between the elements of the reducing and elevating mode, considering the component with the maximum value in the design. As an example, the capacitor 1 value is 3.69μF in elevating mode and 1.92μF in reducing mode, so the one with the higher value is chosen. In these cases the higher value is the one determined, however, due to the existing commercial values, the elements are replaced by components with approximate values.

3.3.1. SEPIC variable input

Following the component definitions shown in Table 3, a simulation of the SEPIC converter was run in PSIM using a variable power supply as shown in Figure 7 to plot plots of input voltage, output voltage, second capacitor and converter output current.

Figure 7 Simulation of SEPIC converter in PSIM

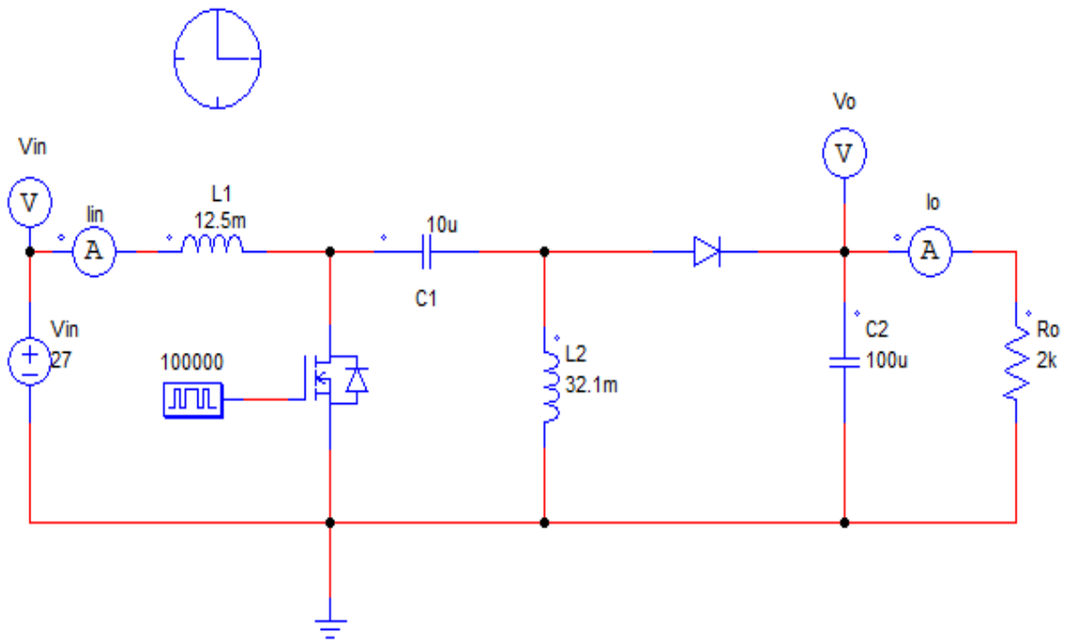

Source: Own Elaboration

As an example of SEPIC converter operation in boost mode, a duty cycle of 0.64 and a maximum input voltage of 27V are considered, as shown in Graph 1. In this case the output and second capacitor voltages (V_c)) are equal, resulting in an output current (I_{out}) of 24.06mA for a voltage of 48.31V.

Graph 1 Behavior of the SEPIC converter in boost mode with variable source in PSIM

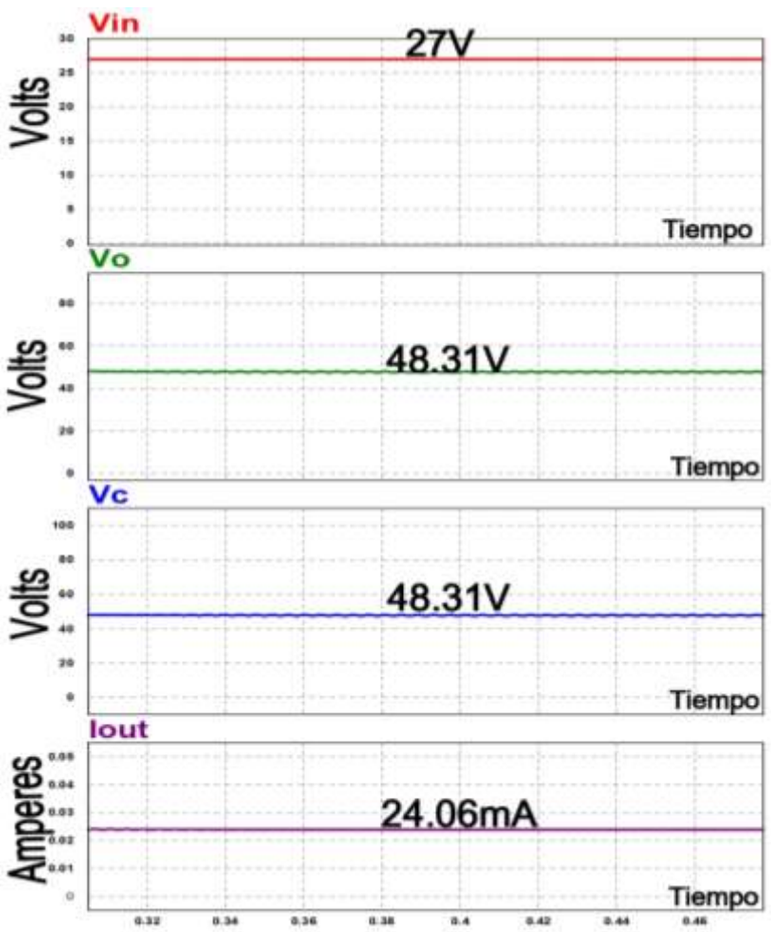

Source: Own Elaboration

As an example of operation of the SEPIC converter in step-down mode, a duty cycle of 0.30 and a maximum voltage of 27V were considered, obtaining the same voltage in the second capacitor and in the output resulting in a value of 11.58V and an I_{out} of 5.79mA, as shown in Graph 2.

Graph 2 Behavior of the SEPIC converter in step-down mode with variable source in PSIM

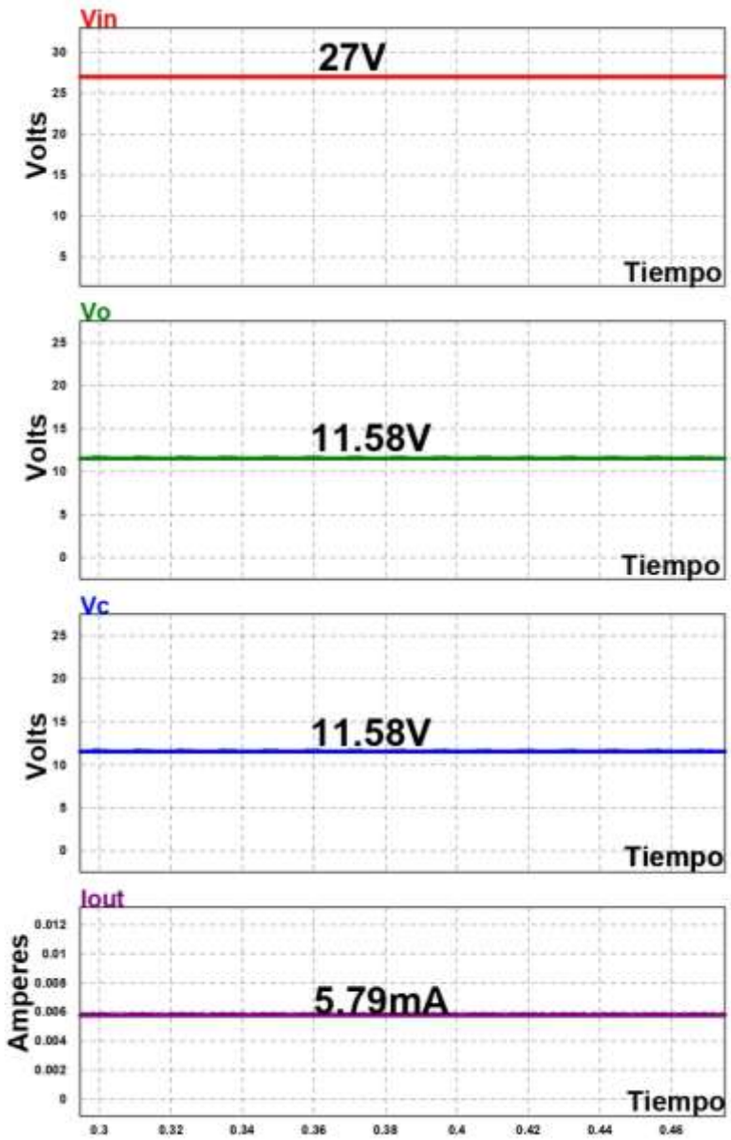

Source: Own Elaboration

On the other hand, a simulation of a SEPIC converter with variable power supply was developed in Proteus software, shown in Figure 8. This software incorporates the control stage designed in Section 3.2, performing several behavior tests by adjusting the frequency to 100kHz and the duty cycle according to its operation mode.

Figure 8 Simulation of the SEPIC converter with control stage in Proteus

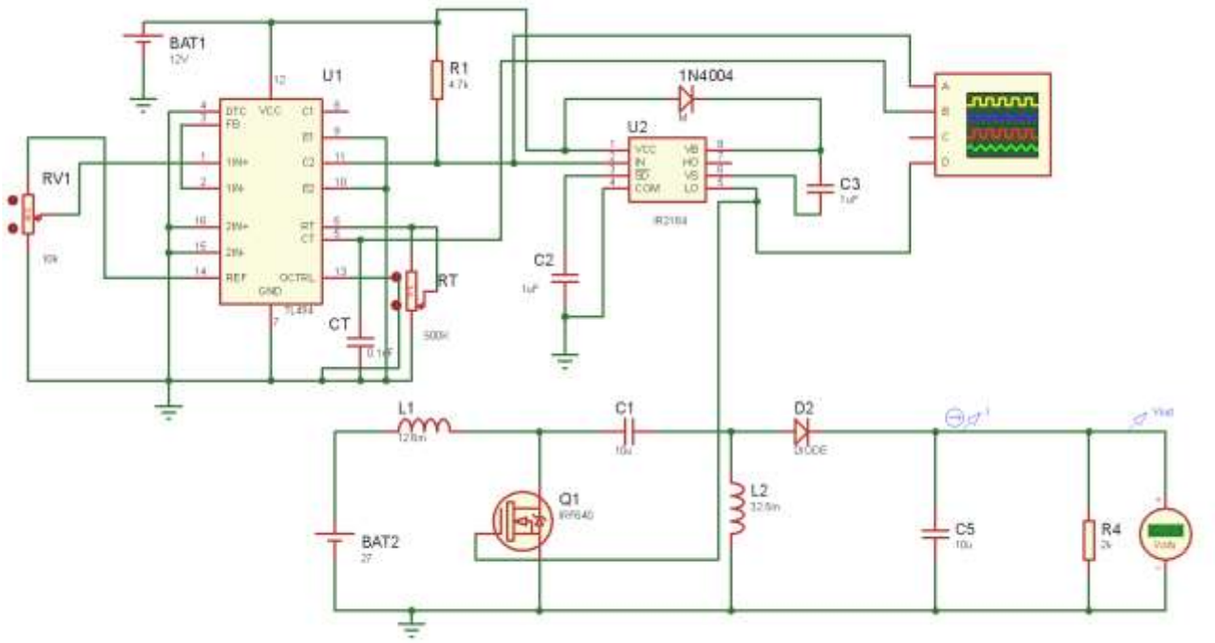

Source: Own Elaboration

As shown in Figure 9, one of the tests performed to a SEPIC converter in reducer mode was performed with a V_{in} associated to the series array of solar cells with a voltage of $27V$ shown in the C channel signal and a duty cycle at 30% shown in the yellow signal, the V_{out} of the converter is 13.8V and an I_{out} $6.88mA$.

Figure 9 Reducer mode behavior in Proteus

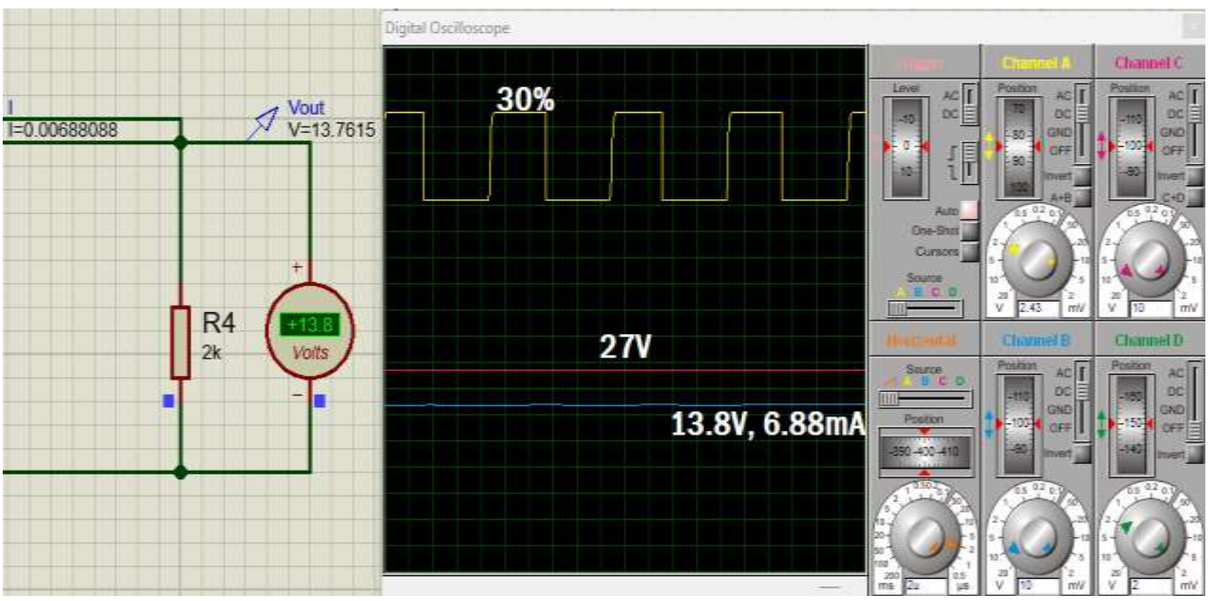

Source: Own Elaboration

Figure 10 shows a test of the converter in boost mode with a V_{in} of $9V$ and a duty cycle of 64%, resulting in an output of 18.53V and an I_{out} $9.27mA$.

Figure 10 Boost mode behavior in Proteus

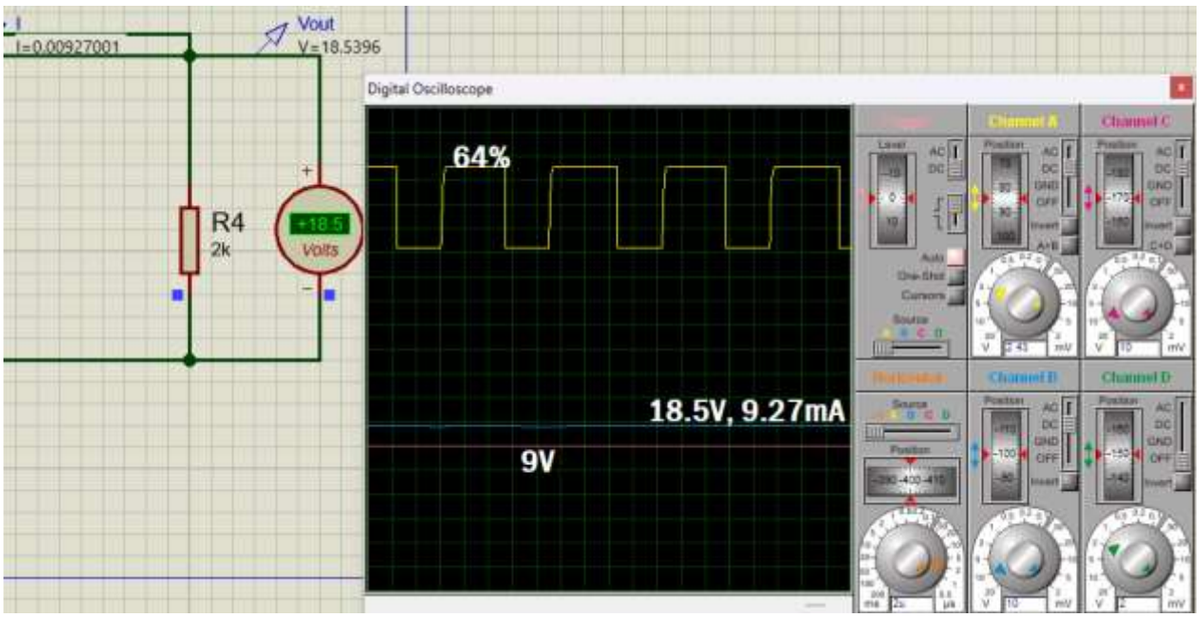

Source: Own Elaboration

3.3.2 SEPIC with solar cells

The incorporation of the series array to the electrical circuit of the SEPIC converter in PSIM considered the characteristics of the cells, including the maximum voltage of the array. Figure 11 shows the SEPIC converter with a power supply coming from the solar cell array, thus eliminating the variable power supply.

Figure 11 SEPIC converter with solar cells in PSIM

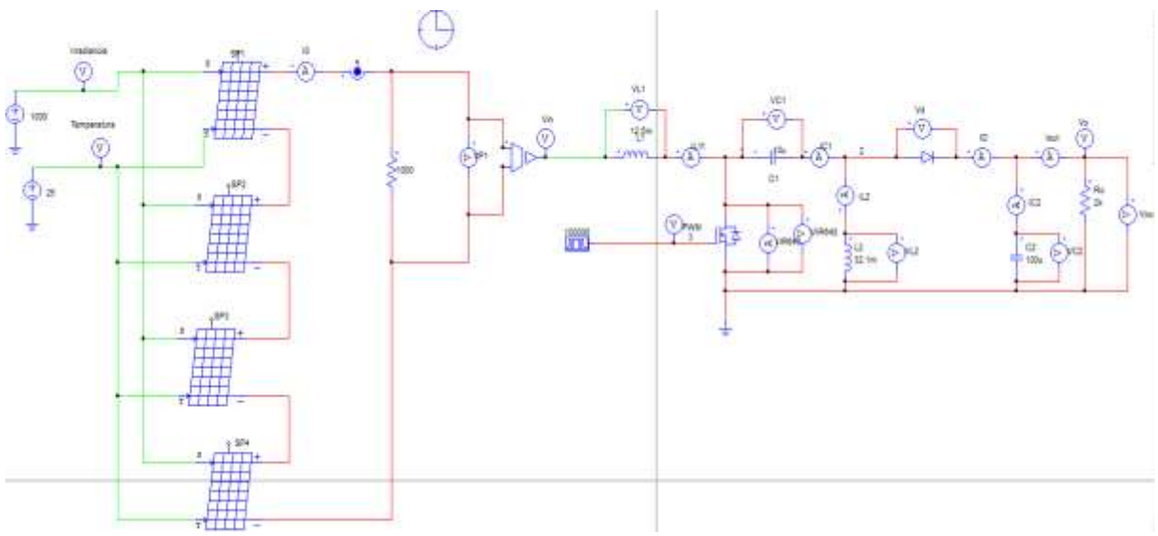

Source: Own Elaboration

Figure 14 shows the operation of the SEPIC converter in elevating mode with the array of solar cells in series, likewise the square signal was adjusted with a frequency of 100kHz and a duty cycle of 0.64, which produced a V_{in} of 27.37V of the array of cells, an I_{out} of 24.34mA and a V_{out} de 48.68 V.

Graph 3 SEPIC behavior in riser mode in PSIM

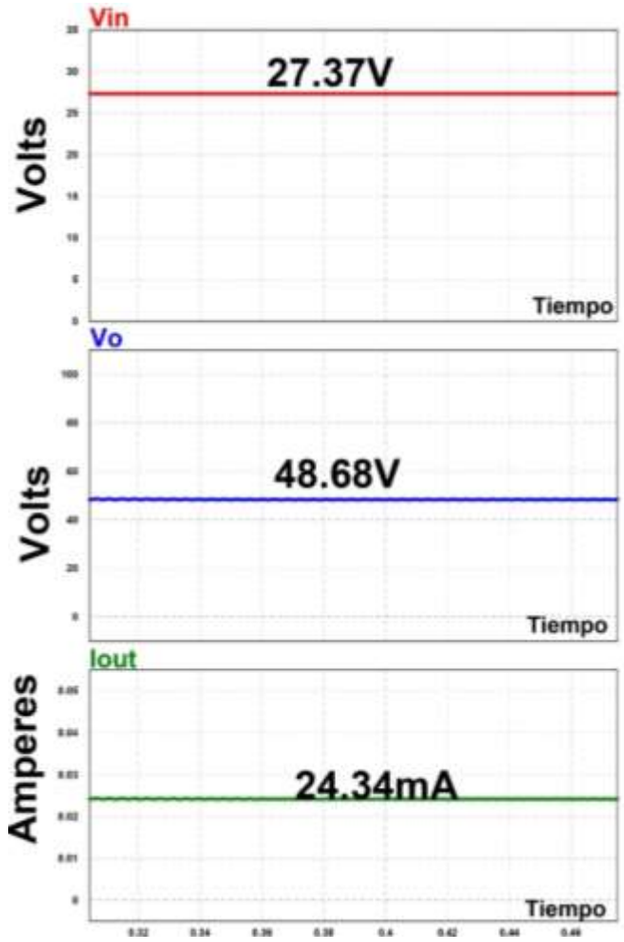

Source: Own Elaboration

As shown in Graph 3, the SEPIC converter in geared mode obtained an input voltage of 27.37V, an I_{out} of 6.02mA and V_o of 12.05V, for the simulation the duty cycle was reset to 30%.

In step-down mode, the SEPIC converter received an input voltage of 27.37V, an 12.05V of 6.02mA and V_o of 12.05V, as shown in Figure 4, readjusting the duty cycle to 30%.

Graph 4 SEPIC behavior in step-down mode in PSIM

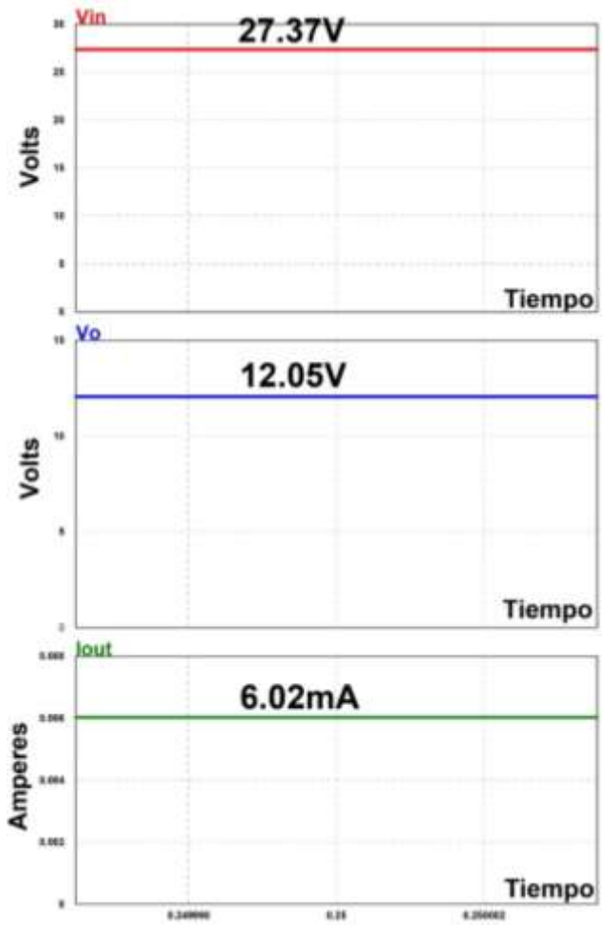

Source: Own elaboration

3.4. IT System

The purpose of the IT-based monitoring system is to use software and hardware elements to sample the SEPIC converter during its operation.

Figure 12. IT System Diagram in draw.io.

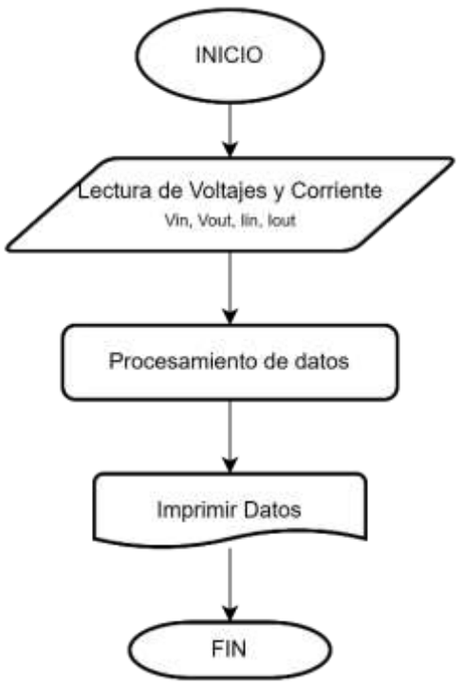

Source: Own Elaboration

As shown in the flowchart in Figure 12, the system was implemented from Arduino code version 2.0.1 and data reading using two types of sensors known as voltage sensor and current sensor model ACS712 to take readings of V_{in}, V_{out},, input current I_{in}, I_{out}. Once the data is received, it is processed in Excel software using Stream Data tool, the data saved in Excel was used to create a .TBL file to get a graph of the readings in PSIM.

4. Results

4.1 Array array of solar cells

Figure 13 shows the physical layout of the SM141K10LV solar cells arranged on a wooden base with an inclination of 16.78° degrees. The tilt of the cells was determined with respect to the tilt angle methods in Mexico around latitude.

Figure 13 Construction of series array of SM141K10LV cells.

Source: Own Elaboration

The solar cell array was subjected to several operational tests at different times of the day, to observe different irradiance captures. For example, on May 5, 2023 at 12:20 pm a maximum voltage of 21.31V was reached and at 18:30 pm a minimum voltage of 0.69V was reached. Another test performed on April 21, 2023 at 13:00 pm reached a maximum voltage of 25.71V as shown in Figure 14, but reached a minimum voltage of 0.10V at 18:50 pm.

Figure 14 Series array voltage test

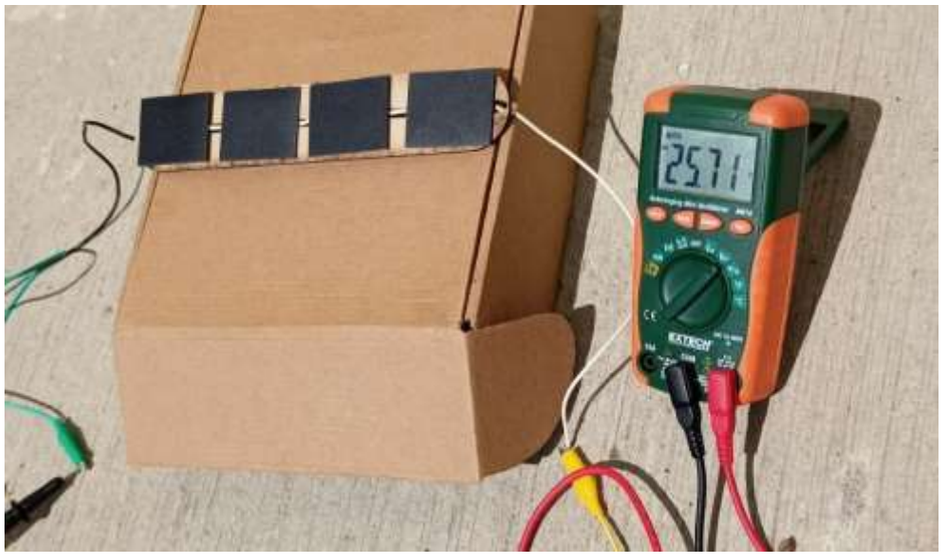

Source: Own Preparation

4.2 Behavior of SEPIC converter with variable power source

A variable power supply was used in the SEPIC converter to observe the physical behavior of the converter at various voltages, in its two step-up and step-down modes, considering for both a frequency of 100 kHz.

Figure 15, shows the physical implementation of the PWM control stage and the SEPIC converter implemented on a phenolic board with THT construction technology and one dimension environment the power systems of a nanosatellite.

Figure 15 PWM control circuit and SEPIC converter

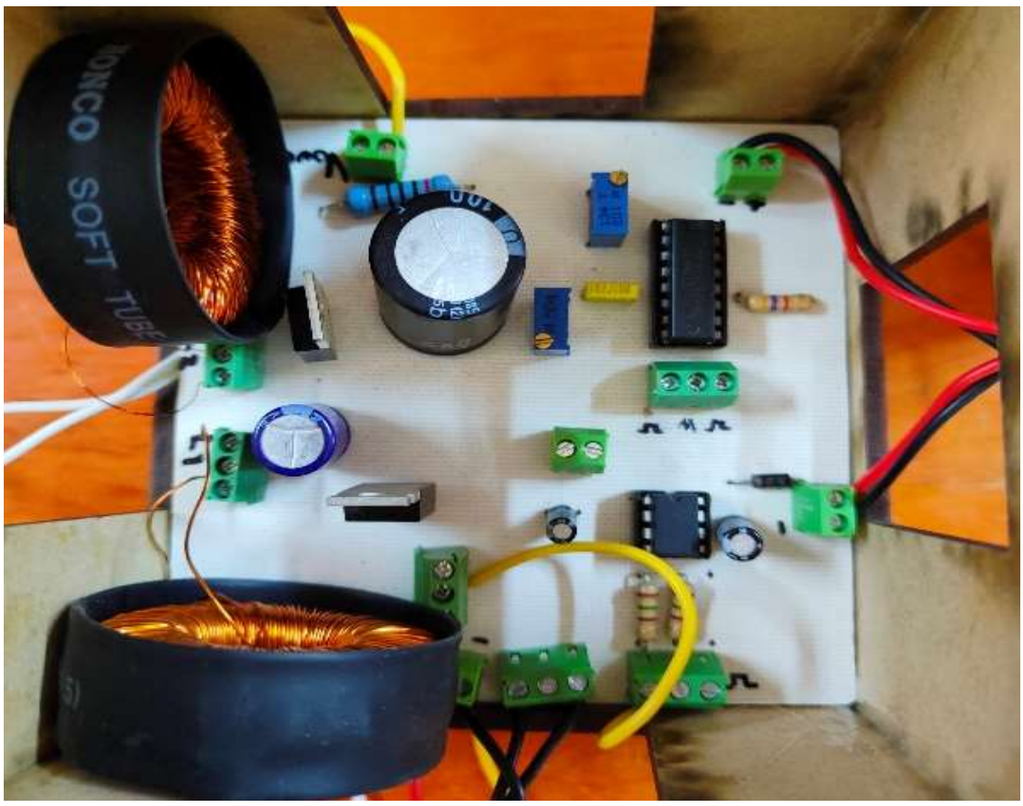

Source: Own Elaboration

The oscilloscope screen was captured at the output of the IR2184 controller, whose signal is shown in Figure 16, the driver output is a PWM modulation with operating conditions of 100kHz in frequency and a duty cycle of 63.9%.

Figure 16 PWM control in elevator mode seen in oscilloscope

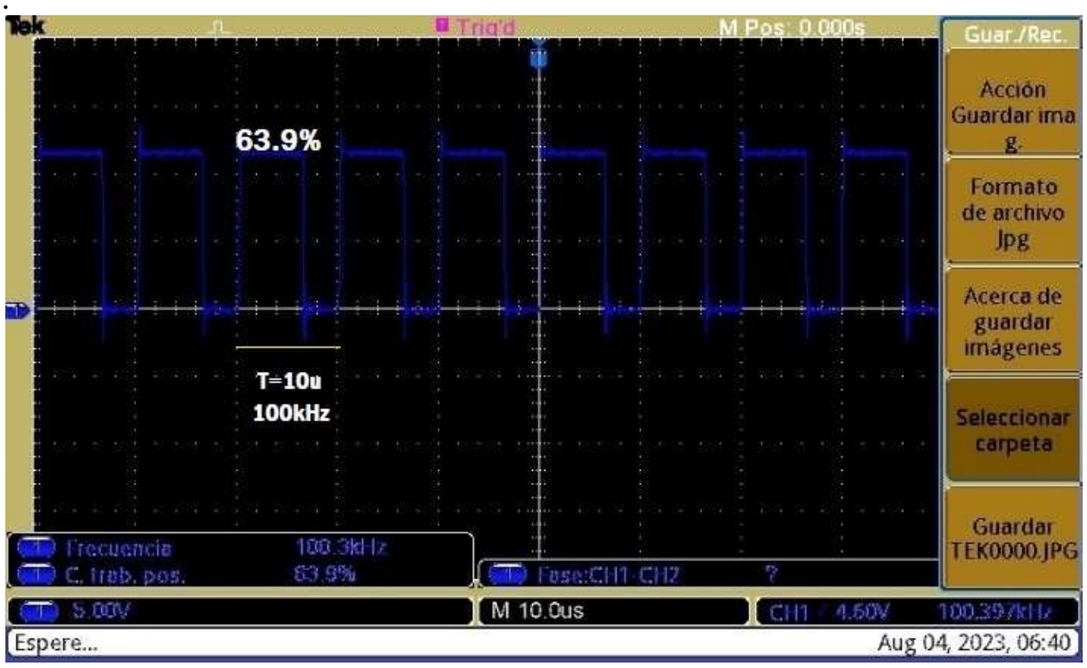

Source: Own Elaboration

For the operation of the converter in step-down mode, the duty cycle was adjusted to 30% of the PWM control, performing several tests. The first voltage reduction test was performed with a low input voltage of 8.28V, which resulted in a V_{out} of 4.13V, as shown in Figure 17.

Figure 17 Reducer mode with low V_{in}seen in oscilloscope

Source: Own Elaboration

In Figure 18, the variable power supply was modified by increasing it to 26.1*V*, giving 11.8*V* at the output of the SEPIC converter.

Figure 18 Reducer mode with 26.1V seen in oscilloscope

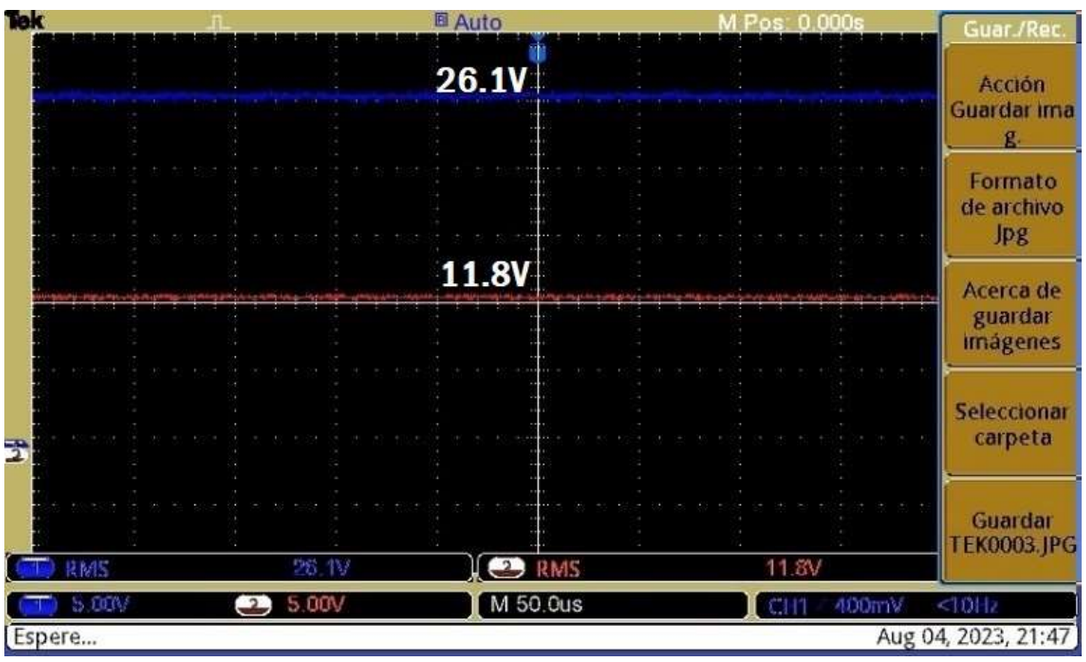

Source: Own Elaboration

To operate in lift mode of the SEPIC converter, the control stage was reset with a duty cycle of 63.9% and 23*V* input, resulting in a lift voltage of 44.7*V*, as shown in Figure 19.

Figure 19 Lifting mode with 23V seen in oscilloscope

Source: Own Elaboration

Among several tests of the SEPIC converter in boost mode, the second test was performed with a V_{in} of 7.90V, obtaining a V_{in} of 14.7V, as shown in Figure 20.

Figure 20 Boost mode at 7.90V seen in oscilloscope

Source: Own Preparation

4.3. Behavior of SEPIC converter with solar cells

The physical structures of the design stage such as the series array of solar cells, the control stage and the SEPIC converter, were integrated to allow performance testing by incorporating TI.

Figure 21 SEPIC converter and solar cell array

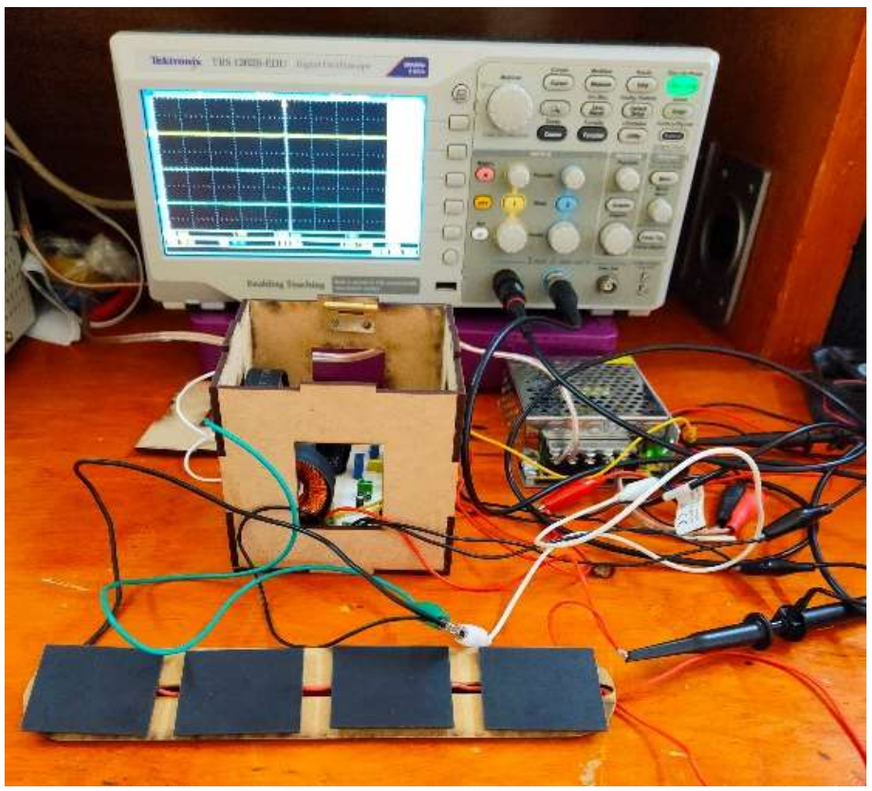

Source: Own Elaboration

As shown in Figure 21, the series circuit was integrated into the power input of the converter, while the PWM control power supply came from a separate 12*V* power supply.

Figure 22 shows the TI system connected to a SEPIC converter with the hardware part contained on a phenolic board consisting of an arduino nano, two ACS712 current sensors, two voltage sensors designed with a voltage divider. The software used was Excel with the Stream Data tool to collect, store the data to be measured. Subsequently, the data were used to obtain the behavioral graphs.

Figure 22 Physical incorporation with the hardware of the IT system

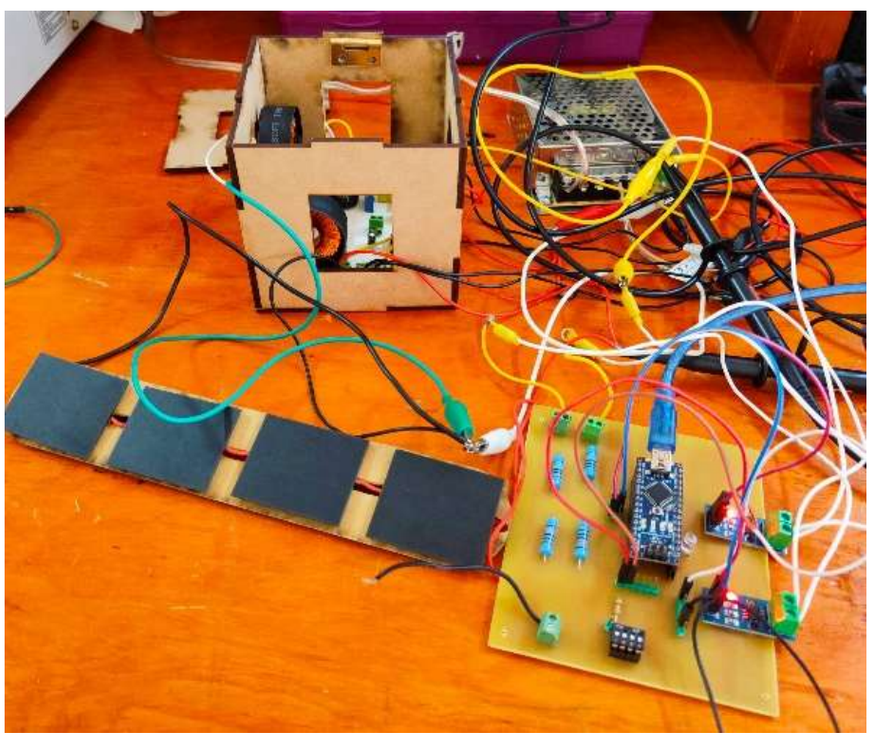

Source: Own Elaboration

4.4 Use Case I

One of the use cases was carried out on June 18, 2023, from 6:30 am to 18:30 pm, with a sampling every 10 minutes, in elevator mode by the SEPIC converter. Solar irradiance was measured with the Fluke IRR1-SOL instrument which allows measuring irradiance and temperature of photovoltaic cells with a 16.5° degree inclination on the instrument. The monitoring system also recorded V_{in}, V_o, I_{in} and I_{out} measurements. Power, temperature, and voltage graphs were generated using data collected from the TI system and the Fluke IRR1-SOL instrument. As shown in Graph 5, the measurement started at 6:30 am with an irradiance of 17 W/m^2, as the day progressed the maximum power point (M_{ppt}) was reached at 11:20 am with a value of 1018 W/m^2, however, by 18:30 pm there was a low irradiance of 10W/m^2.

Graph 5 Irradiance on June 18, 2023 at PSIM

Source: Own Elaboration

Graph 6 shows that the temperature started at 15.1°C at 6:30am, and reached 37.8°C at 11:20am at the point of maximum power. The temperature rose and fell throughout the day, reaching 16.4°C at 18:30pm.

Graph 6 Temperature on June 18, 2023 at PSIM

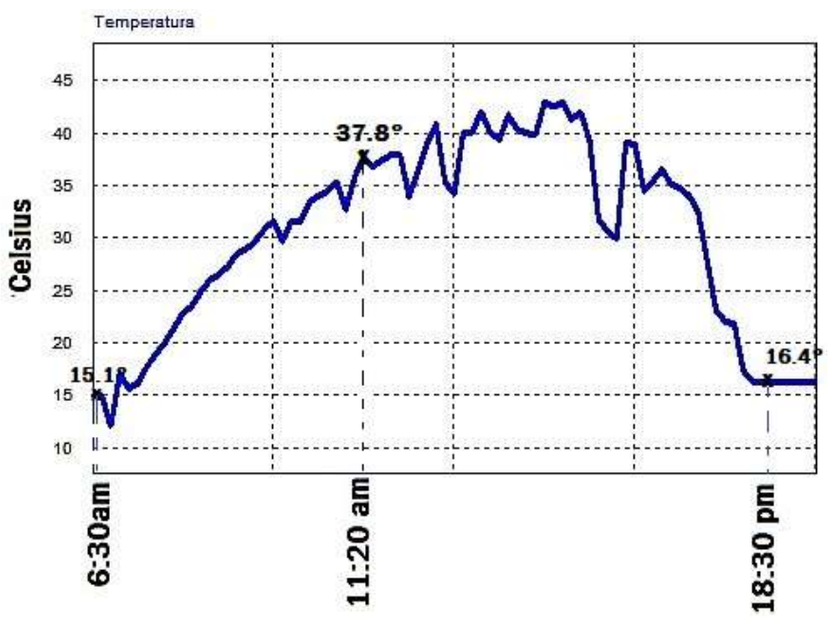

Source: Own Elaboration

The input voltage recorded at the beginning of the samples was very low due to the irradiance of the sun, so 0.35V was obtained. The voltage detected at 9:00 am was 17.85V, while the voltage obtained at the point of maximum power was 21.51V, as shown in Graph 7.

Graph 7 Input voltage on June 18, 2023 at PSIM

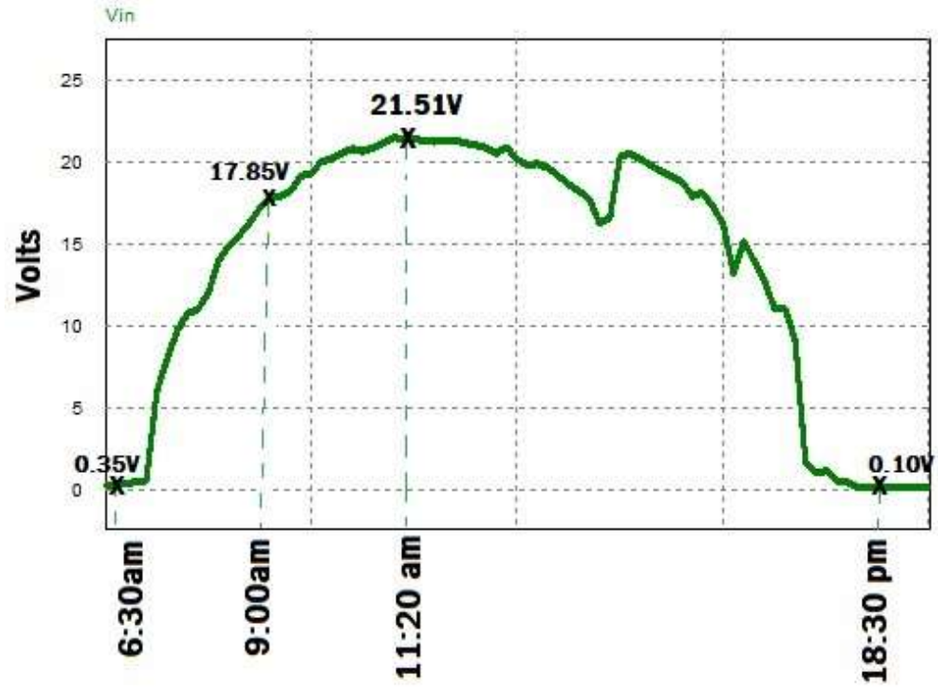

Source: Own Elaboration

As shown in Graph 8, we obtain a V_{out} at the output of the SEPIC converter. The first high voltage measurement was 1V and at M_{ppt} the V_{out} reached 41.72V, while at 17:00pm the V_{out} was 32.76V.
Graph 8. Output voltage on June 18, 2023 at PSIM.

Source: Own Elaboration

4.5 Use Case II

The second use case was carried out on June 26, 2023 from 6:30 am to 18:30 pm, sampling every 10 minutes the SEPIC converter in step-down mode. The irradiance was measured with the Fluke IRR1-SOL with an inclination of 16.1° degrees, with the data collected by the IT system and the Fluke, the power, temperature, $V_{out}$and V_{in} graphs were made. As shown in Graph 9, the values began to be measured at 6:30 am with an irradiance of 8 W/m^2, reaching the M_{ppt} of 1007 W/m^2 at 11:40 am, by the end of the samples the irradiance was 9 W/m^2.

Graph 9 Irradiance on June 26, 2023 at PSIM

Source: Own Elaboration

In Graph 10, the initial temperature of the samples started at 14°C, reaching 38.8°C at M_{ppt}. The maximum temperature of the day was obtained at 12:40pm with a value of 43.9°C.

Graph 10 Temperature on June 26, 2023 at PSIM

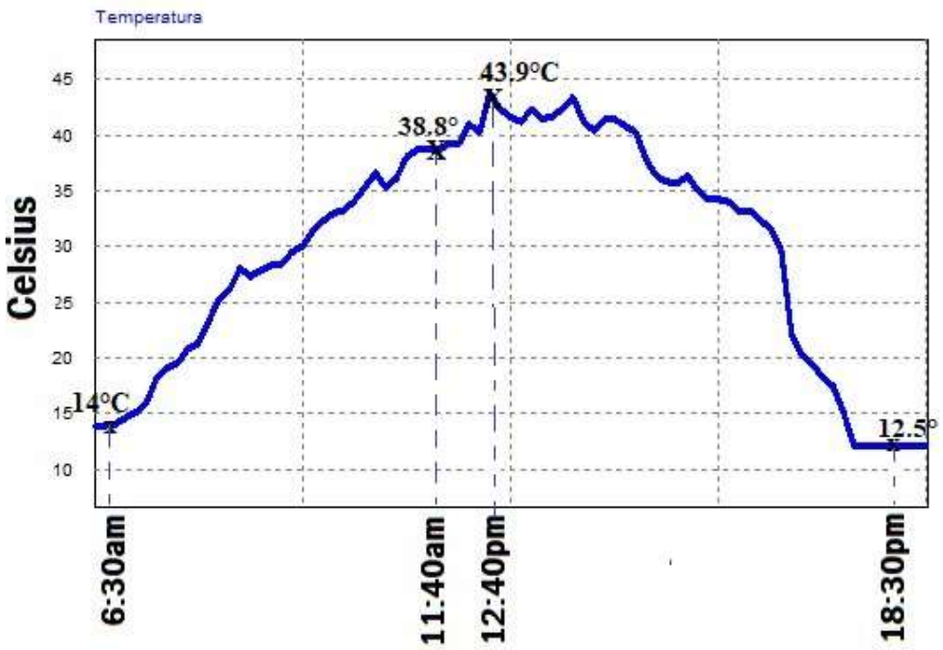

Source: Own Elaboration

The V_{in} started at 1.23V due to the low irradiance at the beginning of the samples, however, at the point of maximum power the V_{in} was 21.34V, by 18:30pm the voltage obtained was very low with a value of 0.83V, as shown in Graph 11.

Graph 11 Input voltage on June 26, 2023 in PSIM

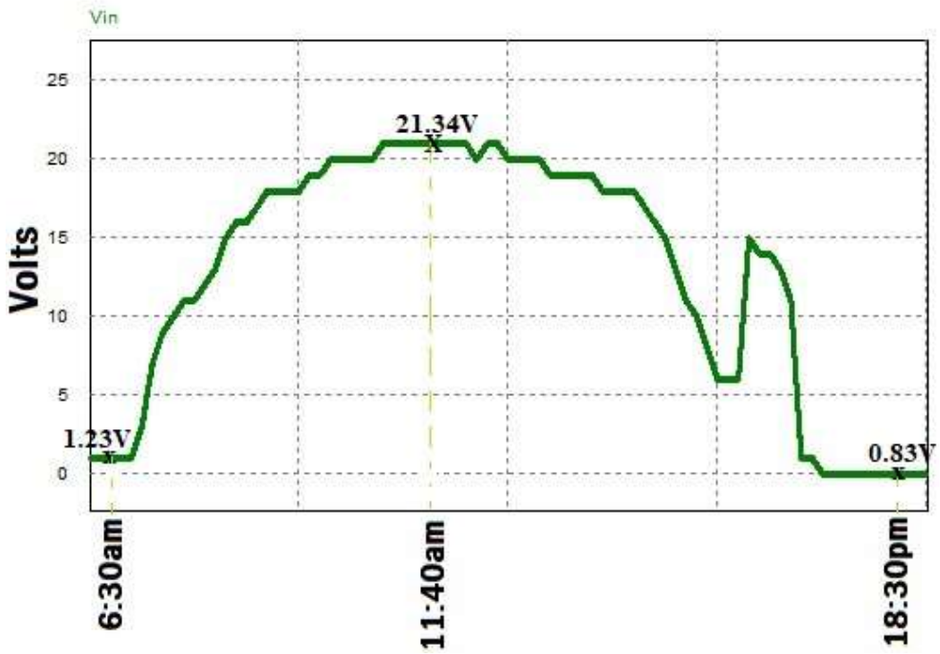

.

Source: Own Elaboration

As shown in Graph 12, the first reduced output voltage was 0.85V, for the maximum power point the V_{out} reached 11.88V, while the V_{out} measured at 16:50pm was 5.75V.

Graph 12 Output voltage on June 26, 2023 at PSIM

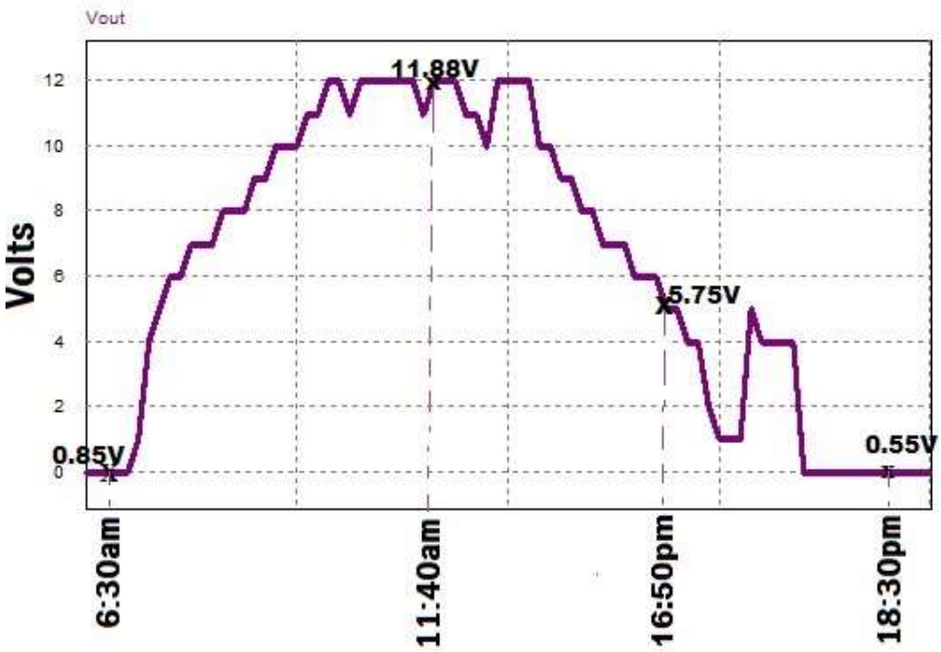

Source: Own Elaboration

5. Acknowledgements

The authors of this work are grateful for the support provided by the University of Ixtlahuaca and the School of Engineering for the development of this project.

6. Conclusions

The prototype fulfills the main objective of this work, which was to develop a solar energy monitoring system using a SEPIC converter for nanosatellite applications. However, the development of the prototype went through a series of stages that led to an analytical analysis to obtain the precise components, as well as simulations of its operation individually, to later unify all the stages to obtain a monitoring system with a SEPIC converter and a power supply from solar cells.

As can be seen in the results, the stages were tested individually until a total incorporation, for this purpose, operation tests were carried out with variable power supplies and the solar cell module tested on different days in May, June and July 2023. Taking into account the spatial conditions, measurement tests were performed using tilt characteristics related to the latitudinal positions where the tests were performed.

The use cases foreseen for this work are in elevating and reducing mode, we observed that the irradiance during the measurement day reached values higher than those estimated by the simulations, the simulated irradiance was 1000 W/m^2 and the values measured by the Fluke instrument were up to 1018 W/m^2. Also the maximum temperature between the two predicted cases was between 30 and 48 degrees Celcius being higher than that given by the simulation.

Depending on the conditions during the course of a day, there will be changes such as partial shadows caused by clouds, objects, among others, causing that the solar cells will not receive the same light intensity, the input voltage will not always be the maximum of the solar cells and the amount of solar radiation and the temperature will not be constant.

However, the tests started with a low voltage until it reached a maximum voltage and then decreased again until it showed very low irradiance levels in the afternoon-evening. Based on the tests conducted on different days, it was confirmed that the SEPIC converters maintain their step-up and step-down characteristics even in static series connection. In this regard, physical considerations regarding the dimensions and characteristics of the nanosatellites were evaluated in the overall context of the project. For example, key design features were the mounting of the PWM controller and SEPIC converter on a small phenolic plate in proportion to a nanosatellite in addition to the integration of solar cells..

7. Referencias

Abella, M. A. (2021). Sistemas Fotovoltaicos. *CIEMAT*, 20-59.

Céspedes, J. E. (2012). Celdas fotovoltaicas de alta eficiencia y sistema de paneles solares del CubeSat

Colombia 1. *Universidad Distrital Francisco José de Caldas*, 50.

Espacial, M. A. (2020). Ingeniería de Sistemas Espaciales. *AEM*, 46.

Fernández, M. S., & López, L. F. (2004). *The Use of satellites in the Earth and Life Sciences.* Enseñanza de las Ciencias de la Tierra.

Flores, C. R. (2017). Analisis de un convertidor DC/DC destinado al almacenamiento híbrido de energía. *ETSII-UPM*, 16-28.

López, R. A. (2018). Asistente para el Diseño y Simulación de Convertidores DC-DC en Lazo Cerrado. 62-68.

Montero, J. A. (2013). Modelado, diseño y simulación del convertidor CC-CC SEPIC para la utilización en sistemas portátiles(PDAs). 50-127.

Patel, M. R. (2004). *Spacecraft Power Systems.* United States of America: CRC Press.

Plá, J. (2017). Una miradas a las celdas solares espaciales. *CNEA-CONICET*, 2.

Saucedo, J. (2016). Caracterización estructural y eléctrica de celdas fotovoltaicas de doble y triple capa. *Centro de investigación en materiales avanzados*.

Tamasi, J. M. (2003). Celdas Solares para Uso Espacial:Optimización de Procesos y Caracterización. *Universidad nacional de general san martín*, 120-188.